

Magnetization reversal via the formation of stripe domains in ultrathin Fe films on Cu(100)

G. Meyer, A. Bauer, T. Crecelius, I. Mauch, and G. Kaindl

Institut für Experimentalphysik, Freie Universität Berlin, Arnimallee 14, 14195 Berlin-Dahlem, Germany

(Received 19 September 2003; published 9 December 2003)

We report on a study of the magnetic-field induced magnetization-reversal process in ultrathin films of Fe/Cu(100) in the vicinity of the spin-reorientation transition. Magnetic domain patterns were visualized by scanning near-field magneto-optical microscopy *in situ* in ultrahigh vacuum and in presence of external magnetic fields. We find that for films with perpendicular anisotropy, magnetization reversal happens via formation of stripe domains with sub- μm stripe widths. Observed hysteresis effects are explained by pinning of stripes.

DOI: 10.1103/PhysRevB.68.212404

PACS number(s): 75.70.-i, 68.37.Uv, 75.60.-d

The occurrence of stripe-domain phases is a general phenomenon in systems with competing long-range and short-range interactions.¹ Well-known examples are magnetic stripe domains in thin magnetic films that are stabilized by a strong, but short-range exchange interaction in combination with long-range magnetic dipole fields. Of particular interest are two-dimensional systems, such as ultrathin magnetic films, where various stripe-domain phases have been identified.^{2,3} For ultrathin films with perpendicular magnetic anisotropy, stripe domains have been found in the vicinity of spin-reorientation transitions (SRT's).⁴⁻¹⁰ Such SRT's are often attributed to a dependence of the magnetic anisotropy on temperature and film thickness which can be caused, e.g., by a strong surface anisotropy that differs substantially from the bulk. Or, they can be caused by structural transitions that occur during film growth. In the vicinity of a SRT, magnetic anisotropies and, as a consequence, domain-wall energies are small, a fact that renders microdomain phases, such as stripe-domain patterns, energetically favorable, in particular if the reduction in dipole energy exceeds the energy necessary to form domain walls.⁴ Binding energies of stripe-domain patterns are relatively small, i.e., it will take only weak magnetic fields (< 50 Oe) to transform such a domain pattern to a homogeneously magnetized state.^{4,7,9} In case of ultrathin films of Fe/Cu(100), grown at 80 K, a SRT from out-of-plane to in-plane magnetization has been reported to occur at about 4 monolayers (ML).¹¹

Magnetization processes in external magnetic fields in the vicinity of a SRT have been studied predominantly via the magneto-optical Kerr effect (MOKE). In only a few cases could the magnetization curves be modeled in a quantitative way by considering both homogeneously magnetized and stripe-domain phases.¹² In most cases, the magnetization curves exhibit strong hysteresis effects, and so far it has not become clear what (metastable) states and what domain structures occur and how they transform in a magnetization-reversal process.^{13,14} Therefore, a better understanding of these processes can only be achieved by magnetic-domain imaging¹⁵ with sub- μm lateral resolution in external magnetic fields. Most magnetic microscopy techniques that provide sufficiently high spatial resolution, such as various types of electron microscopies,^{6,8,16,17} however, cannot readily be applied in the presence of an external magnetic field. Magneto-optical microscopy (Kerr or Faraday microscopy),

on the other hand, is well suited for magnetic-field dependent domain imaging, but its resolution is diffraction limited, and hence insufficient to resolve stripe domain patterns.

In the present work, we report on an application of a newly developed UHV scanning near-field optical microscope (SNOM), in combination with MOKE, to study magnetic micro-domain patterns and magnetization-reversal processes in low-temperature-grown ultrathin films of Fe/Cu(100). In this way, magnetic contrast is achieved with lateral resolution beyond the diffraction limit of conventional optical microscopy.^{18,19} By using a Sagnac interferometer for monitoring the magneto-optical effects,²⁰ we demonstrate that the lateral resolution and the Kerr-rotation sensitivity are both high enough to image stripe domains in ultrathin films.

The experiments were performed in an UHV system that includes a chamber for sample preparation, a scanning tunneling microscope (STM), and a chamber allowing MOKE, Kerr microscopy, and SNOM measurements.²¹ The latter is equipped with a liquid-He flow cryostat for variable sample temperatures between 20 and 450 K, and a rotatable *in situ* electromagnet for magnetic fields up to 1500 Oe to be applied either parallel or perpendicular to the sample surface.

The iron films were prepared by vapor deposition of Fe onto a clean Cu(100) single-crystal surface kept at 80 K with subsequent annealing at temperatures up to 350 K.¹⁴ A quartz microbalance served as monitor of the deposition rate with an accuracy of $\pm 20\%$. Depending on film thickness with respect to the critical thickness of the SRT, Fe/Cu(100) films have the easy axis of magnetization either perpendicular or parallel to the film plane.¹¹ When raising the sample temperature, a reversible SRT from out-of-plane to in-plane magnetization is generally observed for films that had been annealed at elevated temperatures prior to the measurements.⁵

The SNOM used here is operated in the shared-aperture mode, i.e., the sample is locally illuminated by a tapered glass fiber tip, which also serves to collect and the reflected light. A laser diode ($\lambda = 670$ nm; power output: 1 mW) serves as light source. The polar Kerr effect is monitored by a custom-built Sagnac interferometer, which—in combination with SNOM—has proven to be highly sensitive to magneto-optical effects, while being inherently insensitive to polarization changes from nonmagnetic origin.^{20,21} Magnetic-domain images are obtained with this Sagnac-

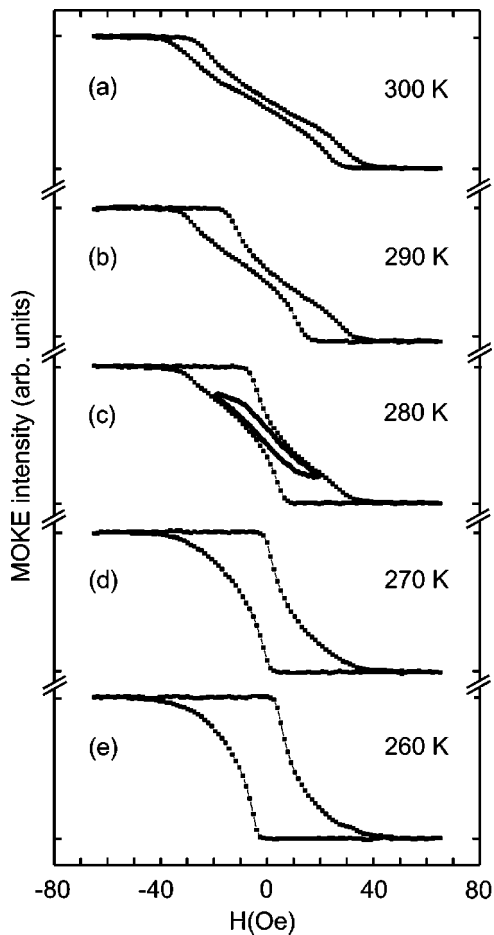


FIG. 1. Polar MOKE hysteresis loops recorded for a 4.2-ML Fe/Cu(100) film at five different temperatures upon annealing at 300 K. In (c), an inner loop is additionally shown.

SNOM by scanning the glass fiber tip at a distance of $\cong 50$ nm across the sample surface and locally measuring the magneto-optical effect. The strong dependence of the intensity of the collected light on the tip-to-sample distance is exploited here for distance control, with the advantage that the tip-to-sample distance can be adjusted to larger values than in the commonly used shear-force distance-control mode.²² In this way, the risk of tip crashes is strongly reduced, while the lateral resolution does not noticeably decrease. With this setup, we have achieved a Kerr-rotation sensitivity of $350 \mu\text{rad}$ and a lateral resolution slightly better than 300 nm, i.e., less than half the wavelength of the laser light. Higher resolution can be achieved with shorter-wavelength light or with a coated fiber tip; the latter, however, will lead to a reduction in signal intensity.

All SNOM measurements reported here were preceded by MOKE and Kerr-microscopy studies since these are less time consuming, but still provide an overview of magnetization and domain patterns on a rougher scale. Figure 1 displays a set of polar MOKE hysteresis loops recorded for a 4.2-ML Fe/Cu(100) film at five different temperatures. With increasing temperature, a gradual transition from a square-like hysteresis loop to one with almost vanishing remanence is clearly visible. A similar behavior was found for other

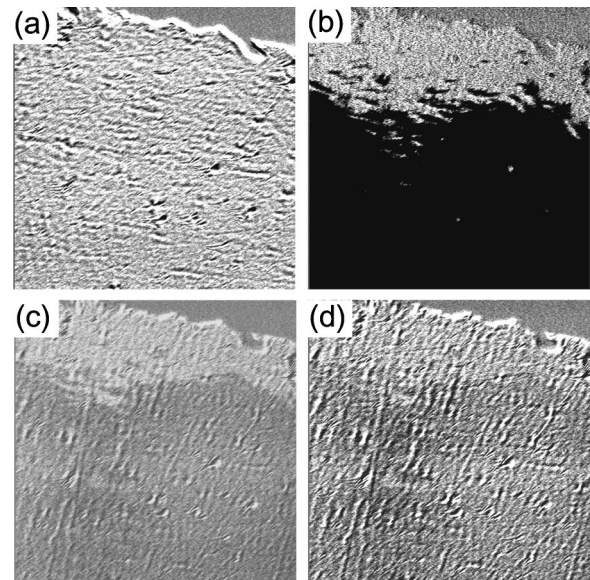


FIG. 2. Series of four images ($550 \mu\text{m} \times 550 \mu\text{m}$) of 4.2-ML Fe/Cu(100) at a temperature of 150 K, in a changing magnetic field taken with the Kerr microscope: (a) Homogeneously out-of-plane magnetized sample; (b) taken during domain growth at $H = H_c$; (c) taken at a reduced magnetic field ($0 < H < H_c$); (d) taken in a reverse magnetic field ($-H_c < H < 0$). The homogeneously gray-shaded areas in the upper-right corners of all four images originate from the nonmagnetic sample holder. Note that the hysteresis loop of this sample is similar to the one of Fig. 1(c). Due to a lower annealing temperature (205 K) of the present film, the SRT is shifted, however. After image (b) was recorded the magnetic field was reduced, i.e., (c) and (d) correspond to an inner hysteresis loop. As a consequence, the darker areas in the images (b), (c), and (d) reflect a reduced net magnetization.

ultrathin-film systems exhibiting a spin-reorientation transition.⁹ The loops are made up of two parts: (i) a square-like part with uniform out-of-plane magnetization up to a critical magnetic field H_c , at which a rapid change of magnetization occurs; (ii) sections where the magnetization changes gradually over a wider magnetic-field range. The latter resemble magnetization curves measured at elevated temperatures [see Fig. 1(a)].

As shown previously by Kerr microscopy and reproduced in the present work (see Fig. 2; compare with Ref. 14, Fig. 3), nucleation of magnetic domains and subsequent growth by domain-wall displacement sets in at H_c , until finally the entire film is transformed to a single magnetic state. This state, however, is not characterized by a uniform out-of-plane magnetization (as expected for a film with large perpendicular anisotropy and a squarelike hysteresis loop), but rather by a reduced net magnetization. With increasing magnetic field, the net magnetization increases up to saturation (out-of-plane magnetization). Note that in previous Kerr-microscopy work, the resolution was not sufficient to resolve the magnetic domain pattern of this phase. It was argued that in addition to a microdomain state, a uniform canted magnetization would also be consistent with the experimental data.¹⁴

As shown in Fig. 3, the results of the present Sagnac-

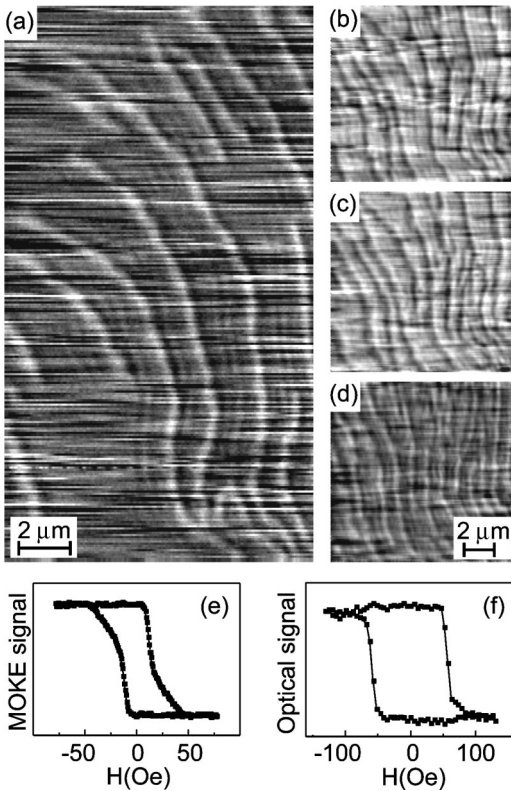


FIG. 3. Stripe-domain patterns, recorded by Sagnac-SNOM, of the same 4.2-ML Fe/Cu(100) film as in Fig. 2 at a temperature of 200 K: (a) In remanence after the fully-magnetized film had been exposed to a reverse magnetic field of about 30 Oe; (b)–(d) three images of the same sample area (the minor displacements are caused by drift) recorded subsequently in external magnetic fields of (b) -15 Oe, (c) 0 Oe, and (d) $+15$ Oe; (e) hysteresis loop recorded of a macroscopic sample area by polar MOKE; (f) hysteresis loop at a microscopic position recorded by Sagnac-SNOM. In (f), a linear background caused by Faraday effect in the glass fiber was subtracted.

SNOM study with sufficient lateral resolution clearly prove that this phase is a microdomain state with alternating up- and down-magnetized stripes. The bright stripes in Fig. 3(a) have a width of $a_{\text{ex}} = (380 \pm 30)$ nm, a value that can be compared with the results of calculations by Yafet and Gyorgy⁴ and by Berger and Erickson:¹² According to Eq. (37) in Ref. 4, the width of a stripe a depends sensitively on the anisotropy constant f . Furthermore, there is a relation between f and the saturation field H_0 at which the transition between the microdomain state and the uniformly out-of-plane magnetized state occurs (see Fig. 2 in Ref. 12). The only further parameter, on which a depends, is the normalized exchange constant R , assumed to be $R = 140$ for Fe.^{4,12} We derive $H_0 = (45 \pm 5)$ Oe from the corresponding polar MOKE hysteresis loop shown in Fig. 3(e), which then leads to $f = 1.022 \pm 0.004$ (Ref. 12) and $a = (350 \pm 50)$ nm, in excellent agreement with the measured stripe width a_{ex} .

In the following, we shall discuss the transformation of stripe-domain patterns in external magnetic fields. By inspecting the Sagnac-SNOM image in Fig. 3(a), which was recorded in remanence (i.e., zero external magnetic field),

one notices that the net magnetization does not vanish as one might expect for zero magnetic field in thermal equilibrium. This is consistent with inner hysteresis loops recorded by polar MOKE that exhibit finite remanent magnetization [see Fig. 1(c)]. Obviously, the existence of an energy barrier, caused, e.g., by local inhomogeneities in the structure or morphology of the film, prevents a reversible transformation of the microdomain pattern. Instead of spontaneously forming a stripe-domain state, followed by a continuous transformation in a changing magnetic field, nucleation of stripes with reversed magnetization is required, which subsequently grow in a mazelike fashion, presumably due to thermally activated steps (Barkhausen jumps).

We would like to mention that the domain image in Fig. 3(a) has some resemblance with simulations performed by Arlett *et al.*²³ for a two-dimensional dipolar Ising model, where—in the presence of a magnetic field—a break-up of the minority stripes into elongated islands was found. Since pinning of stripes was not taken into account, hysteresis effects were absent, leading to a vanishing net magnetization of the calculated domain pattern in remanence.

The assumption of a thermally activated magnetization process is supported by the fact that the saturation field increases with decreasing temperature [compare Figs. 1(b)–1(e)]. For a reversible process, the opposite behavior would be expected: At lower temperatures, the enhanced perpendicular anisotropy would result in smaller binding energies of microdomain states leading to a smaller saturation field.¹² The magnetization curves at elevated temperatures, on the other hand, exhibit less hysteresis [see Fig. 1(a)], and their shapes correspond to a reversible transition between a stripe-domain phase and out-of-plane magnetization with a diverging slope at the saturation field.¹² At these higher temperatures, we expect a diminished influence of pinning on the magnetization-reversal process.

In Figs. 3(b)–3(d), the transformation of the magnetic-domain pattern in a changing magnetic field can be followed. It is striking that the stripe domains do not move freely when the magnetic field is changed, but are pinned to certain positions. Pinning of stripes has recently also been reported for a temperature-dependent transformation of stripe domain patterns.³ It is caused by inhomogeneities of the magnetic anisotropy and/or the thickness of the film, which can be expected from defects of the substrate such as, e.g., polishing scratches. The net magnetization changes either by nucleation of new stripes [compare the images of Figs. 3(b) and 3(c)], or by sudden changes of the stripe widths, with the broad stripes turning narrower and vice versa. The latter process explains the apparent contrast inversion in Figs. 3(c), 3(d). Locally recorded microscopic hysteresis loops exhibit a squarelike shape [see Fig. 3(f)], which suggests that magnetization reversal takes place locally by a single Barkhausen jump. It is interesting to note that the widths of minority stripes [white stripes in Figs. 3(a), 3(d); black stripes in Figs. 3(b), 3(c)] remain almost constant in an external magnetic field, an observation that is in agreement with theoretical⁷ and recent experimental results.¹⁶

The changes in net magnetization that result from transformations of the stripe-domain pattern explain the observed

contrast changes in Kerr-microscope images (see Fig. 2, and Ref. 14) as well as the gradual magnetization changes in the corresponding hysteresis loops. The observation of two-dimensional growth of the stripe-domain pattern indicates that growth is taking place via defect-mediated branching of stripes. Such branching as well as various types of dislocations³ and deviations from a parallel alignment can be clearly seen in Fig. 3.

In summary, by combining MOKE, Kerr microscopy, and Sagnac-SNOM results for ultrathin films of Fe/Cu(100) in the vicinity of the SRT, we have obtained a better understanding of the formation and dynamics of magnetic stripe-domain patterns in external magnetic fields. Pinning of

stripes due to defects at the interface plays an essential role and must be taken into account in theoretical simulations. Note that the Sagnac-SNOM already provides a lateral resolution beyond the diffraction limit. While the UHV Sagnac-SNOM is a relatively simple, compact, and inexpensive setup, it would certainly take a major effort to achieve comparable resolution in UHV with a conventional optical microscope.

This work was supported by the Deutsche Forschungsgemeinschaft, Sfb-290/TPA6. A.B. acknowledges the support of the Deutsche Forschungsgemeinschaft within the Heisenberg program.

-
- ¹M. Seul and D. Andelmann, *Science* **267**, 476 (1995).
²A. Abanov, V. Kalatsky, V.L. Pokrovsky, and W.M. Saslow, *Phys. Rev. B* **51**, 1023 (1995).
³O. Portmann, A. Vaterlaus, and D. Pescia, *Nature (London)* **422**, 701 (2003).
⁴Y. Yafet and E.M. Gyorgy, *Phys. Rev. B* **38**, 9145 (1988).
⁵D.P. Pappas, K.-P. Kämper, and H. Hopster, *Phys. Rev. Lett.* **64**, 3179 (1990).
⁶R. Allenspach and A. Bischof, *Phys. Rev. Lett.* **69**, 3385 (1992).
⁷A.B. Kashuba and V.L. Pokrovsky, *Phys. Rev. B* **48**, 10 335 (1993).
⁸M. Speckmann, H.P. Oepen, and H. Ibach, *Phys. Rev. Lett.* **75**, 2035 (1995).
⁹A. Berger and H. Hopster, *Phys. Rev. Lett.* **76**, 519 (1996).
¹⁰C.S. Arnold, D.P. Pappas, and A.P. Popov, *Phys. Rev. Lett.* **83**, 3305 (1999).
¹¹S. Müller, P. Bayer, C. Reischl, K. Heinz, B. Feldmann, H. Zillgen, and M. Wuttig, *Phys. Rev. Lett.* **74**, 765 (1995).
¹²A. Berger and R.P. Erickson, *J. Magn. Magn. Mater.* **165**, 70 (1997).
¹³F. Baudelet, M.-T. Lin, W. Kuch, K. Meinel, B. Choi, C.M. Schneider, and J. Kirschner, *Phys. Rev. B* **51**, 12 563 (1995).
¹⁴E. Mentz, A. Bauer, T. Günther, and G. Kaindl, *Phys. Rev. B* **60**, 7379 (1999).
¹⁵M.R. Freeman and B.C. Choi, *Science* **294**, 1484 (2001).
¹⁶H.J. Choi, W.L. Ling, A. Scholl, J.H. Wolfe, U. Bovensiepen, F. Toyama, and Z.Q. Qiu, *Phys. Rev. B* **66**, 014409 (2002).
¹⁷R.J. Phaneuf and A.K. Schmid, *Phys. Today* **56**, 50 (2003).
¹⁸E. Betzig, J.K. Trautman, R. Wolfe, E.M. Gyorgy, P.L. Finn, M.H. Kryder, and C.H. Chang, *Appl. Phys. Lett.* **61**, 142 (1992).
¹⁹T.J. Silva, S. Schultz, and D. Weller, *Appl. Phys. Lett.* **65**, 658 (1994).
²⁰B.L. Petersen, A. Bauer, G. Meyer, T. Crecelius, and G. Kaindl, *Appl. Phys. Lett.* **73**, 538 (1998).
²¹G. Meyer, T. Crecelius, G. Kaindl, and A. Bauer, *J. Magn. Magn. Mater.* **240**, 76 (2002).
²²R. Brunner, A. Bietsch, O. Hollricher, and O. Marti, *Rev. Sci. Instrum.* **68**, 1769 (1997).
²³J. Arlett, A.P. Whitehead, A.B. MacIsaac, and K. De'Bell, *Phys. Rev. B* **54**, 3394 (1996).